and anthropogenic forcing factors (for example, land-use change, forest fires, sulphate aerosol concentrations and nitrogen deposition). However, our results indicate that it will be essential to accurately represent previously neglected carbon-cycle feedbacks if we are to successfully predict climate change over the next 100 years. □

Methods

Ocean carbon-cycle model

The inorganic component of HadOCC has been extensively tested as part of the Ocean Carbon Cycle Intercomparison Project; it was found to reproduce tracer distributions to an accuracy consistent with other ocean GCMs[24]. The biological component treats four additional ocean fields: nutrient, phytoplankton, zooplankton and detritus[8]. The phytoplankton population changes as a result of the balance between growth, which is controlled by light level and the local concentration of nutrient, and mortality, which is mostly as a result of grazing by zooplankton. Detritus, which is formed by zooplankton excretion and by phyto- and zooplankton mortality, sinks at a fixed rate and slowly remineralizes to reform nutrient and dissolved inorganic carbon. Thus both nutrient and carbon are absorbed by phytoplankton near the ocean surface, pass up the food chain to zooplankton, and are eventually remineralized from detritus in the deeper ocean. The model also includes the formation of calcium carbonate and its dissolution at depth (below the lysocline).

Terrestrial carbon-cycle model

TRIFFID (top-down representation of interactive foliage and flora including dynamics) has been used offline in a comparison of dynamic global vegetation models[11]. Carbon fluxes for each vegetation type are calculated every 30 minutes as a function of climate and atmospheric CO_2 concentration, from a coupled photosynthesis/stomatal-conductance scheme[25,26], which utilizes existing models of leaf-level photosynthesis in C_3 and C_4 plants[27,28]. The accumulated fluxes are used to update the vegetation and soil carbon every 10 days. The natural landcover evolves dynamically based on competition between the vegetation types, which is modelled using a Lotka–Volterra approach and a tree–shrub–grass dominance hierarchy. We also prescribe some agricultural regions, in which grasslands are assumed to be dominant. Carbon lost from the vegetation as a result of local litterfall or large-scale disturbance is transferred into a soil carbon pool, where it is broken down by microorganisms that return CO_2 to the atmosphere. The soil respiration rate is assumed to double for every 10 K of warming[29], and is also dependent on the soil moisture content[30]. Changes in the biophysical properties of the land surface[5], as well as changes in terrestrial carbon, feed back onto the atmosphere.

Received 6 January; accepted 26 September 2000.

1. Houghton, J. T. *et al.* (eds) *Climate Change 1995: The Science of Climate Change* (Cambridge Univ. Press, Cambridge, 1996).
2. Schimel, D. *et al.* in *Climate Change 1995: The Science of Climate Change* Ch. 2 (eds Houghton, J. T. *et al.*) 65–131 (Cambridge Univ. Press, Cambridge, 1995).
3. Sarmiento, J., Hughes, T., Stouffer, R. & Manabe, S. Simulated response of the ocean carbon cycle to anthropogenic climate warming. *Nature* **393,** 245–249 (1998).
4. Cao, M. & Woodward, F. I. Dynamic responses of terrestrial ecosystem carbon cycling to global climate change. *Nature* **393,** 249–252 (1998).
5. Betts, R. A., Cox, P. M., Lee, S. E. & Woodward, F. I. Contrasting physiological and structural vegetation feedbacks in climate change simulations. *Nature* **387,** 796–799 (1997).
6. Enting, I., Wigley, T. & Heimann, M. *Future Emissions and Concentrations of Carbon Dioxide; Key Ocean/Atmosphere/Land Analyses* (Technical Paper 31, Division of Atmospheric Research, CSIRO, Melbourne, 1994).
7. Gordon, C. *et al.* The simulation of SST, sea ice extents and ocean heat transports in a version of the Hadley Centre coupled model without flux adjustments. *Clim. Dyn.* **16,** 147–168 (2000).
8. Palmer, J. R. & Totterdell, I. J. Production and export in a global ocean ecosystem model. *Deep-Sea Res.* (in the press).
9. Wilson, M. F. & Henderson-Sellers, A. A global archive of land cover and soils data for use in general circulation climate models. *J. Clim.* **5,** 119–143 (1985).
10. Zinke, P. J., Stangenberger, A. G., Post, W. M., Emanuel, W. R. & Olson, J. S. *Worldwide Organic Soil Carbon and Nitrogen Data* (NDP-018, Carbon Dioxide Information Center, Oak Ridge National Laboratory, Oak Ridge, Tennessee, 1986).
11. Cramer, W. *et al.* Global response of terrestrial ecosystem structure and function to CO_2 and climate change: results from six dynamic global vegetation models. *Glob. Change Biol.* (in the press).
12. VEMAP Members. Vegetation/ecosystem modelling and analysis project: comparing biogeography and biogeochemistry models in a continental-scale study of terrestrial responses to climate change and CO_2 doubling. *Glob. Biogeochem. Cycles* **9,** 407–437 (1995).
13. Longhurst, A., Sathyendranath, S., Platt, T. & Caverhill, C. An estimate of global primary production in the ocean from satellite radiometer data. *J. Plank. Res.* **17,** 1245–1271 (1995).
14. Field, C., Behrenfeld, M., Randerson, J. & Falkowski, P. Primary production of the biosphere: integrating terrestrial and oceanic components. *Science* **281,** 237–240 (1998).
15. Antoine, D., Andre, J.-M. & Morel, A. Oceanic primary production 2. Estimation at global scale from satellite (Coastal Zone Color Scanner) chlorophyll. *Glob. Biogeochem. Cycles* **10,** 57–69 (1996).
16. Tian, H. *et al.* Effects of interannual climate variability on carbon storage in Amazonian ecosystems. *Nature* **396,** 664–667 (1998).
17. Keeling, C. D., Whorf, T., Whalen, M. & der Plicht, J. V. Interannual extremes in the rate of rise of atmospheric carbon dioxide since 1980. *Nature* **375,** 666–670 (1995).
18. Houghton, J. T., Callander, B. A. & Varney, S. K. (eds) *Climate Change 1992: The Supplementary Report to the IPCC Scientific Assessment* (Cambridge Univ. Press, Cambridge, 1992).
19. Nicholls, N. *et al.* in *Climate Change 1995: The Science of Climate Change* Ch. 3 (eds Houghton, J. T. *et al.*) (Cambridge Univ. Press, Cambridge, 1996).
20. Mitchell, J. F. B., Johns, T. C., Gregory, J. M. & Tett, S. F. B. Climate response to increasing levels of greenhouse gases and sulphate aerosols. *Nature* **376,** 501–504 (1995).
21. Wood, R. A., Keen, A. B., Mitchell, J. F. B. & Gregory, J. M. Changing spatial structure of the thermohaline circulation in response to atmospheric CO_2 forcing in a climate model. *Nature* **399,** 572–575 (1999).
22. Sarmiento, J. & Quere, C. L. Oceanic carbon dioxide uptake in a model of century-scale global warming. *Nature* **274,** 1346–1350 (1996).
23. Giardina, C. & Ryan, M. Evidence that decomposition rates of organic carbon in mineral soil do not vary with temperature. *Nature* **404,** 858–861 (2000).
24. Orr, J. C. in *Ocean Storage of Carbon Dioxide, Workshop 3: International Links and Concerns* (ed. Ormerod, W.) 33–52 (IEA R&D Programme, CRE Group Ltd, Cheltenham, UK, 1996).
25. Cox, P. M., Huntingford, C. & Harding, R. J. A canopy conductance and photosynthesis model for use in a GCM land surface scheme. *J. Hydrol.* **212–213,** 79–94 (1998).
26. Cox, P. M. *et al.* The impact of new land surface physics on the GCM simulation of climate and climate sensitivity. *Clim. Dyn.* **15,** 183–203 (1999).
27. Collatz, G. J., Ball, J. T., Grivet, C. & Berry, J. A. Physiological and environmental regulation of stomatal conductance, photosynthesis and transpiration: a model that includes a laminar boundary layer. *Agric. Forest Meteorol.* **54,** 107–136 (1991).
28. Collatz, G. J., Ribas-Carbo, M. & Berry, J. A. A coupled photosynthesis-stomatal conductance model for leaves of C4 plants. *Aust. J. Plant Physiol.* **19,** 519–538 (1992).
29. Raich, J. & Schlesinger, W. The global carbon dioxide flux in soil respiration and its relationship to vegetation and climate. *Tellus B* **44,** 81–99 (1992).
30. McGuire, A. *et al.* Interactions between carbon and nitrogen dynamics in estimating net primary productivity for potential vegetation in North America. *Glob. Biogeochem. Cycles* **6,** 101–124 (1992).

Acknowledgements

We thank J. Mitchell and G. Jenkins for comments on earlier versions of the manuscript. This work was supported by the UK Department of the Environment, Transport and the Regions.

Correspondence and requests for materials should be addressed to P.M.C. (e-mail: pmcox@meto.gov.uk).

Offset of the potential carbon sink from boreal forestation by decreases in surface albedo

Richard A. Betts

Hadley Centre for Climate Prediction and Research, The Met Office, Bracknell, Berkshire RG12 2SY, UK

Carbon uptake by forestation is one method proposed[1] to reduce net carbon dioxide emissions to the atmosphere and so limit the radiative forcing of climate change[2]. But the overall impact of forestation on climate will also depend on other effects associated with the creation of new forests. In particular, the albedo of a forested landscape is generally lower than that of cultivated land, especially when snow is lying[3–9], and decreasing albedo exerts a positive radiative forcing on climate. Here I simulate the radiative forcings associated with changes in surface albedo as a result of forestation in temperate and boreal forest areas, and translate these forcings into equivalent changes in local carbon stock for comparison with estimated carbon sequestration potentials[10–12]. I suggest that in many boreal forest areas, the positive forcing induced by decreases in albedo can offset the negative forcing that is expected from carbon sequestration. Some high-latitude forestation activities may therefore increase climate change, rather than mitigating it as intended.

Perturbations to the balance between radiation absorbed and emitted by the Earth ('radiative forcing') can result from changes in atmospheric chemistry and planetary albedo. A positive 'greenhouse' forcing results from increased atmospheric CO_2 absorbing and re-emitting more of the infrared radiation emitted by the surface[13]; forestation may help to mitigate this by slowing the rise

in atmospheric CO_2 concentrations through carbon sequestration[12], but may also provide a further positive forcing by reducing the surface albedo. Forests are generally darker than open land, particularly when snow is lying, because trees generally remain exposed whereas cultivated land can become entirely snow-covered[3–5]. Snow-free foliage is considerably darker than snow, but even if large quantities of snow are held on the canopy, multiple reflections within the canopy scatter rather than reflect shortwave radiation which also reduces the landscape albedo[4]. Models suggest that the resulting low surface albedo causes boreal and cool-temperate forests to exert a warming influence on climate relative to unforested land[6–9] that may be more important than the effects of their carbon storage[8].

To compare the forcings by albedo change and carbon sequestration due to mid- and high-latitude forestation, I have made spatially explicit calculations of shortwave radiation budget perturbations, considering replacement of agricultural land with forest. I then compare these with the effects of carbon sequestration by calculating the changes in atmospheric CO_2 concentration (and hence changes in carbon stock) that would give the same forcings as those exerted by the local albedo changes. For consistency with carbon sequestration estimates[11], I have considered dense coniferous plantations. These generally have a higher sequestration potential than natural forests at middle and high latitudes.

The radiative forcing due to surface albedo change was simulated with the radiative transfer scheme[14] of the third Hadley Centre Atmosphere Model (HadAM3) (ref. 15). This simulates the Earth's radiation budget with a 3-hour timestep on a global grid of 3.75° longitude by 2.5° latitude, with 19 levels in the vertical. The shortwave radiation budget at each gridpoint is influenced by the simulated surface albedo and also by cloud and water vapour provided by other components of the atmosphere model. The surface albedo depends on the local vegetation and soil types and the depth and temperature of any lying snow[16]; of particular importance here is the inclusion of the effect of vegetation on surface albedo in snowy conditions[6]. The surface albedo α is calculated at each gridpoint as

$$\alpha = \alpha_0 + (\alpha_D - \alpha_0)(1 - e^{-0.2S}) \quad (1)$$

where α_0 is the local albedo in snow-free conditions, S is the snow mass ($kg\,m^{-2}$), and α_D represents the influence of vegetation type and surface temperature $T*$(K) when snow is lying[16]:

$$\alpha_D = \begin{cases} \alpha_s & \text{for } T_* < T_M - \Delta T \\ \alpha_s + 0.3(\alpha_0 - \alpha_s)(T_* - T_M + \Delta T)/\Delta T & \\ & \text{for } T_M - \Delta T \leqslant T_* \leqslant T_M \end{cases} \quad (2)$$

T_M is 273.15 K, and ΔT is 2.0 K. The vegetation-dependent deep-snow albedo parameter α_s provides the upper limit on albedo during deep snow cover, and is much lower for forests than for open land (Table 1). In snowy conditions, α can vary from 0.8 to 0.25 according to whether the local vegetation is farmland or forest.

Two 20-year radiation budget simulations were performed, with different data fields of α_0 and α_s but with the same meteorological inputs. Simulation CONIF used α_0 and α_s for dense, mature, evergreen coniferous forest (Table 1) at points north of 23° N where widespread forest is sustainable[17,18], and simulation CROP used α_0 and α_s for arable cropland (Table 1) at these same points. The simulations calculated the surface albedo for the given vegetation cover using the same patterns of S and $T*$ from a 20-year HadAM3 simulation of present-day climate, and used this to model the shortwave radiation budget using cloud cover and other data again from HadAM3. The simulated outgoing shortwave flux at the tropopause was compared at each gridpoint, and the difference (CONIF–CROP) gave the local shortwave radiative forcing due to a change from cropland to coniferous forest.

In the boreal forest regions, the simulated surface albedo was 0.1–0.3 lower in CONIF than in CROP in the annual mean (Fig. 1a). The difference was greatest in the areas of longest-lasting snow cover, which were generally the farthest north. In temperate regions, the difference ranged from 0.04 to 0.15 depending on snow-cover duration and local soil albedo. The associated annual-mean local shortwave radiative forcing ranged from 3 $W\,m^{-2}$ in temperate regions to over 20 $W\,m^{-2}$ in the boreal forests of eastern Canada and eastern Siberia (Fig. 1b). The spatial maxima of the annual mean albedo and forcing did not coincide, because higher latitudes are sunlit for a shorter time and hence allow less forcing per unit albedo change.

To compare the climatic influence of albedo change with that of carbon sequestration for a given location, the effect of local albedo change on the global mean radiative forcing was found. The change in carbon stock that would give this same global forcing via atmospheric CO_2 change was then calculated. Because the calculations are nonlinear, the results will depend slightly on the scale of the forestation units; here, 1-ha plantations were considered. The contribution F of a plantation to global forcing was found by dividing the local radiative forcing (Fig. 1b) by the Earth's surface area in hectares, and the global-mean atmospheric CO_2 concentration change ΔC which would give the same forcing F was given by[19]

$$F = 5.35\ln(1 + \Delta C/C_0) \quad (3)$$

where C_0 is the 1997 CO_2 concentration, 363.8 p.p.m.v. (ref. 20). ΔC is related to the terrestrial carbon stock change ΔC_T by

$$\Delta C_T = 2(M_c/M_a)m_a\Delta C/C_0 \quad (4)$$

where M_c and M_a are the molecular masses of carbon and dry air, and m_a is the mass of the atmosphere. The factor of 2 accounts for an airborne fraction of emissions of 0.5 (ref. 13), assumed to remain constant over forest growth timescales. Combining equations (1) and

Table 1 Albedo parameter values before and after forestation

Land cover	α_0 (dark soil)	α_0 (medium soil)	α_0 (light soil)	α_s
Arable cropland	0.18	0.19	0.21	0.78
Dense coniferous forest	0.14	0.14	0.15	0.26

Values of snow-free albedo parameter α_0 and deep-snow albedo parameter α_s for arable cropland and dense evergreen coniferous forest. α_0 depends on the albedo of the underlying soil, which varies according to soil type. Soil moisture dependence of α_0 is assumed to be negligible, and dependencies on wavelength and solar zenith angle are also neglected. These values are used along with those for other land surface types to derive α_0 and α_s fields for HadAM3 and the current operational weather forecast models of the Met Office[3,29,30].

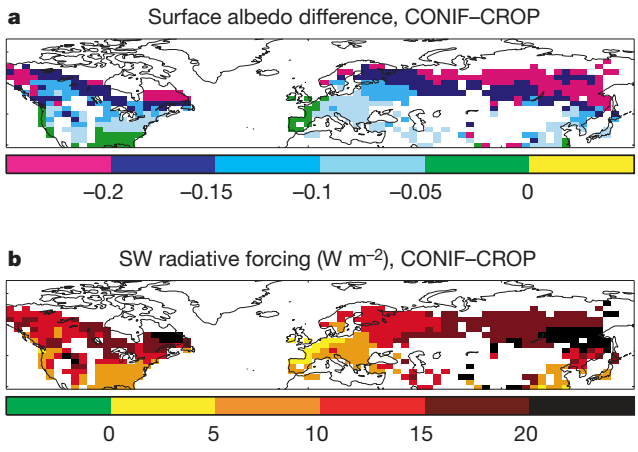

Figure 1 Effects of forestation on the solar radiation budget. **a**, Difference in annual-mean surface albedo α simulated by CONIF and CROP. **b**, Local instantaneous shortwave (SW) radiative forcing at the tropopause due to surface albedo change. At uncoloured gridpoints, vegetation was identical in CONIF and CROP.

(2) to find ΔC_T from F gave the emissions equivalent of the shortwave forcing (EESF). Assuming that α_0 and α_s reach the values given in Table 1 within one forest management rotation period, the EESF can then be compared with sequestration estimates[10–12] (Table 2).

In the boreal forest regions, the replacement of crops with carbon-sequestering forests induced a positive albedo forcing equivalent to the emission of 50–140 t C ha^{-1} (Fig. 2a). The greatest effect was in eastern Siberia, where the EESF was 90–140 t C ha^{-1}. The carbon sequestration potential (SP) in the former Soviet Union is estimated to be 80–120 t C ha^{-1} (Table 2), so if this is appropriate to eastern Siberia then forestation in this region could exert a net warming influence (Fig. 2b). In the intensive agricultural regions of western Russia, the EESF of 80–90 t C ha^{-1} could again largely counteract or overcome the estimated carbon sink (Fig. 2). Similarly in Canada, the EESF was 60–110 t C ha^{-1}, which significantly outweighs the mean sink potential of 60 t C ha^{-1} estimated for most of this region (Fig. 2, Table 2). This suggests that in many boreal forest areas, forestation could therefore exert a net positive radiative forcing of climate, rather than a negative forcing as intended.

The EESF in British Columbia was smaller than the estimated SP (Table 2) because the relatively mild climate leads to less snow cover than elsewhere in Canada and also, presumably, enhances sequestration. However, the albedo change still significantly reduces the net forcing of climate in comparison with that expected from sequestration alone, because the net equivalent stock change (NESC = SP − EESF) is only 60% of the SP (Table 2). Similarly, the NESC for Nordic Europe is only 50% of the SP (Table 2). Carbon accounting[12] would therefore overestimate the associated mitigation of climate change by a factor of approximately two.

In temperate regions, the EESF ranged from 20 to 80 t C ha^{-1} (Fig. 2a). The smallest effects were in western Europe, the western USA and southern China, where infrequent snow cover and/or low soil albedo[17] suppressed the albedo change when the vegetation was modified. The effects were largest where snow lies for a significant part of the year; the EESF reached 80 t C ha^{-1} in the northern USA, and exceeded 100 t C ha^{-1} in the Rocky Mountains, northern China and the fringes of the Tibetan plateau. The area-mean EESF was smaller than the estimated SP in all regions classified here as 'temperate', and for most regions the NESC was 70–90% of the SP (Table 2). The mean NESC for China was only 30% of the SP, the latter being relatively small due to a low growth rate estimate[11] while the mean EESF was high because of large forcings in the north (Fig. 2a). I note that the growth rate given for this region is similar to that for the neighbouring former Soviet Union[11], so may be applicable only to northern China. Latitudinal comparisons with other regions suggest that higher SPs may be more appropriate in southern China, but higher-resolution sequestration estimates will be required to confirm this. Despite such uncertainties, these results show that although temperate forestation should still exert a net negative radiative forcing, the effect cannot be adequately quantified by simple carbon accounting.

These results clearly rely on accurate representation of S, α_0 and α_s. S from HadAM3 agrees with an observation-based monthly climatology[21] to within 10% across most regions in the annual mean. HadAM3 gives more snow than the climatology in parts of Russia, and less in eastern Europe, but the greatest disagreement is in southeastern Canada where the climatology gives around twice as much snow mass as HadAM3. The observation-based snow mass would reduce the EESF by approximately 10–15 t C ha^{-1} in eastern Siberia, but would increase that in eastern Canada by around 15 t C ha^{-1}. Climate and weather simulations using α_0 and α_s as in Table 1 show no evidence of bias attributable to errors in these parameter values for these surface types. However, lower α_s values of

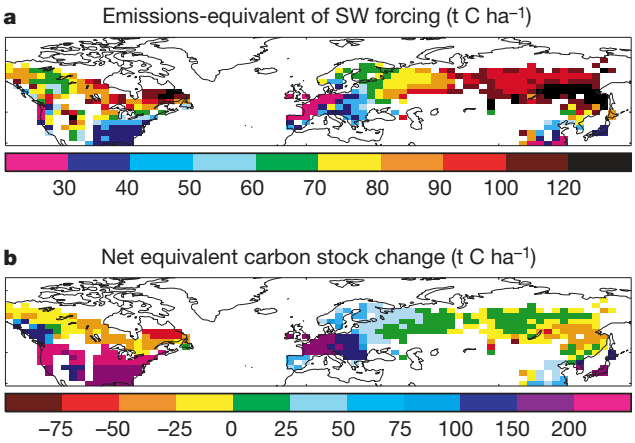

Figure 2 Effects of albedo change on annual-mean global radiative forcing in terms of carbon stock change. **a**, Carbon emissions (t C ha^{-1}) that would provide global radiative forcing equal to that exerted by local surface albedo change due to forestation (EESF). See text for error estimates. **b**, Net changes in equivalent carbon stock (NESC, t C ha^{-1}) considering both sequestration potential (SP) and EESF. SP contribution is from regionally representative values (Table 2) applied across whole regions because higher-resolution data are not available; this results in discontinuities across some region boundaries (for example, the USA/Canada border) where smooth transitions are expected in reality. Where ranges of SP estimates apply, range means are used here. Negative NESC implies a net radiative forcing equivalent to net carbon emission. At uncoloured gridpoints, vegetation was identical in CONIF and CROP.

Table 2 Sequestration and albedo forcings in terms of carbon stock change

Region	Sequestration potential, SP (t C ha^{-1})	Emissions-equivalent of shortwave forcing, EESF (t C ha^{-1})	Net equivalent stock change, NESC (t C ha^{-1})	NESC/SP (%)
Boreal				
Former Soviet Union	80–120	100	–20–20	–30–20
British Columbia	190	80	110	60
Rest of Canada	60	90	–30	–50
Nordic Europe	120	60	60	50
Temperate				
Western Europe	140–280	30	110–250	80–90
Eastern Europe	150	40	110	70
Southern Europe	90	40	50	60
Temperate USA	200–420	70	130–350	70–80
Southern USA	210	40	170	80
China	80	60	20	30
Rest of temperate Asia	200	60	140	70

Column 2 gives ranges of regional estimates of carbon sequestration potential by forestation over one rotation period, based on literature data[10,11]. Coniferous plantations are specified for sequestration estimates in the boreal forest regions, the USA and western Europe[10,11]; for other regions the forest type is unspecified[11] and was assumed here to be coniferous. Sequestration potentials include above- and below-ground biomass, and were estimated here as mean net uptake[10,11] times mean rotation period[10,11]. Rotation periods range from 40 to 80 yr. Nabuurs and Mohren[10] give total system uptake at specified locations representative of major biomes. Nilsson and Schopfhauser[11] give regional values and separate above-ground and below-ground uptake, the latter being in root biomass (20%/19% of total living biomass for boreal/temperate forests[11]), litter (0.32%/2.11% of above-ground biomass[11]), and soil (regionally specific estimates[11]). In column 4, NESC = SP – EESF. Data are rounded to the nearest 10 to avoid misleading precision.

0.10–0.18 have been suggested for dense coniferous forest[4,5]; this would increase the EESF by approximately 25 t C ha^{-1} in the most snow-covered regions.

Here I have considered forestation under present-day conditions, but the effects of future CO_2 rise and climate change are likely to affect the magnitude of both radiative forcing terms, due to dependencies on time-varying quantities such as the atmospheric CO_2 concentration, snow extent and vegetation structure and leafiness. As the atmospheric CO_2 concentration increases, CO_2 fertilization is likely to increase carbon uptake[22] so the magnitude of the negative sequestration forcing should therefore increase, although associated climate changes may exert additional positive or negative effects on sequestration. Warmer temperatures may reduce the extent of snow cover[23], but the leaf area index (LAI) of potential vegetation may increase[24,25], so the albedo forcing could either increase or decrease. The effect of vegetation on surface albedo is not necessarily proportional to biomass, so the net contribution to radiative forcing may not evolve linearly throughout a forest's development; albedo depends on canopy density and architecture, and can become low rapidly, whereas carbon sequestration depends largely on woody biomass which is more gradually accumulated. Other contributions to forcing may also require consideration; for example, the longwave radiation budget could be affected by modified surface emissivity[25], although the sign of such changes is uncertain[25,26].

The work I report here has focused on perturbations to the Earth's radiation budget, which is the fundamental driver of the climate system. Forestation may also influence the climate by modifying the fluxes of heat, moisture and momentum between the land surface and atmosphere. Whereas boreal forests warm their local climate through reduced albedo, tropical forests tend to cool and moisten their local climates by greatly enhancing evaporation. Both may also influence distant regional climates via the atmospheric circulation[9,27]. Assessment of the effect of forestation on climate at a given time in the future will require simulations with a climate model that incorporates vegetation dynamics[25,28] and other atmospheric, terrestrial and oceanic components of the carbon cycle[28], in which forest growth occurs at appropriate rates in relation to changes in atmospheric CO_2 and snow cover. Nevertheless, my results suggest that high-latitude forestation would exert a positive radiative forcing through reduced albedo that in many places could outweigh the negative forcing through carbon sequestration. If afforestation and reforestation are required to decrease radiative forcing rather than simply to reduce net CO_2 emissions, then changes in surface albedo must also be considered. □

Received 10 July; accepted 27 September 2000.

1. UNFCCC *Kyoto Protocol to the United Nations Framework Convention on Climate Change* Art. 3.3 (UNEP/INC/98/2, Information Unit for Conventions, UNEP, Geneva, 1998) <http://www.unfccc.int/resource/docs/convkp/kpeng.pdf>.
2. UNFCCC *United Nations Framework Convention on Climate Change* Art. 2 (UNEP/IUC/99/2, Information Unit for Conventions, UNEP, Geneva, 1999); <http://www.unfccc.int/resource/convkp.html>.
3. Robinson, D. A. & Kukla, G. Albedo of a dissipating snow cover. *J. Climatol. Appl. Meteorol.* **23,** 1626–1634 (1984).
4. Harding, R. J. & Pomeroy, J. W. The energy balance of the winter boreal landscape. *J. Clim.* **9,** 2778–2787 (1996).
5. Sharratt, B. S. Radiative exchange, near-surface temperature and soil water of forest and cropland in interior Alaska. *Agric. Forest Meteorol.* **89,** 269–280 (1998).
6. Thomas, G. & Rowntree, P. R. The boreal forests and climate. *Q. J. R. Meteorol. Soc.* **118,** 469–497 (1992).
7. Bonan, G. B., Pollard, D. & Thompson, S. L. Effects of boreal forest vegetation on global climate. *Nature* **359,** 716–718 (1992).
8. Bonan, G. B., Chapin, F. S. & Thompson, S. L. Boreal forest and tundra ecosystems as components of the climate system. *Clim. Change* **29,** 145–167 (1995).
9. Douville, H. & Royer, J. F. Influence of the temperate and boreal forests on the Northern Hemisphere climate in the Météo-France climate model. *Clim. Dyn.* **13,** 57–74 (1997).
10. Nabuurs, G. J. & Mohren, G. M. J. Modelling analysis of potential carbon sequestration in selected forest types. *Can. J. Forest Res.* **25,** 1157–1172 (1995).
11. Nilsson, S. & Schopfhauser, W. The carbon sequestration potential of a global reforestation program. *Clim. Change* **30,** 267–293 (1995).
12. Watson, R. T. *et al.* (eds) *Land Use, Land-use Change and Forestry* (Cambridge Univ. Press, Cambridge, 2000).
13. Schimel, D. *et al.* in *Climate Change 1995. The Science of Climate Change* Ch. 2 (eds Houghton, J. T. *et al.*) 65–131 (Cambridge Univ. Press, Cambridge, 1995).
14. Edwards, J. M. & Slingo, A. Studies with a flexible new radiation code. I: Choosing a configuration for a large-scale model. *Q. J. R. Meteorol. Soc.* **122,** 689–720 (1996).
15. Pope, V. D., Gallani, M. L., Rowntree, P. R. & Stratton, R. A. The impact of new physical parametrizations in the Hadley Centre climate model - HadAM3. *Clim. Dyn.* **16,** 123–146 (2000).
16. Hansen, J. E. *et al.* Efficient three dimensional global models for climate studies, Models I and II. *Mon. Weath. Rev.* **111,** 609–662 (1983).
17. Wilson, M. F. & Henderson-Sellers, A. A global archive of land cover and soils data for use in general circulation climate models. *J. Climatol.* **5,** 119–143 (1985).
18. Woodward, F. I., Smith, T. M. & Emanuel, W. R. A global land primary productivity and phytogeography model. *Glob. Biogeochem. Cycles* **9,** 471–490 (1995).
19. Myhre, G., Highwood, E. J., Shine, K. P. & Stordal, F. New estimates of radiative forcing due to well mixed greenhouse gases. *Geophys. Res. Lett.* **25,** 2715–2718 (1998).
20. Keeling, C. D. & Whorf, T. P. *Atmospheric CO_2 Concentrations - Mauna Loa Observatory, Hawaii, 1958-1997* (NDP-001, Carbon Dioxide Information Analysis Centre, Oak Ridge, Tennessee, 1998).
21. Willmott, C. J., Rowe, C. M. & Mintz, Y. Climatology of the terrestrial seasonal water cycle. *J. Climatol.* **5,** 589–606 (1985).
22. Cao, M. & Woodward, F. I. Dynamic responses of terrestrial ecosystem carbon cycling to global climate change. *Nature* **393,** 249–252 (1998).
23. Essery, R. Seasonal snow cover and climate change in the Hadley Centre GCM. *Ann. Glaciol.* **25,** 362–366 (1997).
24. Betts, R. A., Cox, P. M., Lee, S. E. & Woodward, F. I. Contrasting physiological and structural vegetation feedbacks in climate change simulations. *Nature* **387,** 796–799 (1997).
25. Levis, S., Foley, J. A. & Pollard, D. Potential high-latitude vegetation feedbacks on CO_2-induced climate change. *Geophys. Res. Lett.* **26,** 747–750 (1999).
26. Kondratyev, K. Y., Korzov, V. I., Mukhenberg, V. V. & Dyachenko, L. N. in *Land Surface Processes in Atmospheric General Circulation Models* (ed. Eagleson, P. S.) 463–514 (Cambridge Univ. Press, Cambridge, 1982).
27. Gedney, N. & Valdes, P. J. The effect of Amazonian deforestation on the northern hemisphere circulation and climate. *Geophys. Res. Lett.* **27,** 3053–3056 (2000).
28. Cox, P. M., Betts, R. A., Jones, C. D., Spall, S. A. & Totterdell, I. J. Acceleration of global warming due to carbon-cycle feedbacks in a coupled climate model. *Nature* **408,** 184–187 (2000).
29. Cox, P. M. *et al.* The impact of new land surface physics on the GCM simulation of climate and climate sensitivity. *Clim. Dyn.* **15,** 183–203 (1999).
30. Posey, J. W. & Clapp, P. F. Global distribution of normal surface albedo. *Geofis. Int.* **4,** 333–348 (1964).

Acknowledgements

I thank S.E. Lee and F.I. Woodward for providing data from the Sheffield University vegetation model, and P.M. Cox, J.M. Edwards, R.L.H. Essery, W.J. Ingram, G.J. Jenkins, J.E. Lovelock, S. Nilsson, I.C. Prentice, P.R. Rowntree, K.P. Shine, P.J. Valdes and D.A. Warrilow for advice, comments and discussion. This work forms part of the Climate Prediction Programme of the UK Department of the Environment, Transport and the Regions.

Correspondence should be addressed to the author (e-mail: rabetts@meto.gov.uk).

An artificial landscape-scale fishery in the Bolivian Amazon

Clark L. Erickson

Department of Anthropology, University of Pennsylvania, 33rd and Spruce Streets, Philadelphia, Pennsylvania 19104-6398, USA

Historical ecologists working in the Neotropics argue that the present natural environment is an historical product of human intentionality and ingenuity, a creation that is imposed, built, managed and maintained by the collective multigenerational knowledge and experience of Native Americans[1,2]. In the past 12,000 years, indigenous peoples transformed the environment, creating what we now recognize as the rich ecological mosaic of the Neotropics[3–6]. The prehispanic savanna peoples of the Bolivian Amazon built an anthropogenic landscape through the construction of raised fields, large settlement mounds, and earthen causeways[7,8]. I have studied a complex artificial network of hydraulic earthworks covering 525 km^2 in the Baures region of Bolivia. Here I identify a particular form of earthwork, the zigzag structure, as a fish weir, on the basis of form, orientation, location, association with other hydraulic works and ethnographic analogy.